Reprinted from Nature, Vol. 310, No. 5975, pp. 316-318, 26 July 1984

How a gap junction maintains its structure

Jochen Braun, James R. Abney & John C. Owicki

Department of Biophysics and Medical Physics,
University of California, and Division of Biology and Medicine,
Lawrence Berkeley Laboratory, Berkeley, California 94720, USA

In gap junctions, identical membrane proteins are linked up in pairs (dyads) that bridge the extracellular space between two apposed cell membranes[1,2]. Typically, several thousand of these dyads are aggregated in the plane of the membranes and form a junctional plaque with a distinct boundary. The question thus arises as to what maintains the dyads in an aggregated state. From a statistical mechanical analysis of the positions of dyads in a freeze-fracture electron micrograph, we report here that the aggregates are not maintained by an attractive force between pairs of dyads, but probably by the minimization of the repulsive force between apposed membranes. On the basis of this analysis we present a model for the structure of mature gap junctions as well as certain aspects of the formation and disassembly of gap junctions.

Freeze-fracture electron microscopy of tissue that has been rapidly frozen by the method of Heuser and Reese[3] reveals to a good approximation the *in vivo* distribution of intramembrane particles[4]. Figure 1 shows a part of the electron micrograph of a gap junction in mouse liver that forms the basis of our analysis. As there is strong evidence against cytoskeletal attachment to dyads[5–7], it is plausible to assume that dyads are free to move laterally in the two junctional membranes and that aggregation into plaques is an equilibrium condition that reflects attractive forces among dyads. But before such a 'fluid mosaic' model can be satisfactory, the nature of the forces that maintain the aggregated state must be elucidated.

There is a rigorous and well developed theory of fluids that relates the forces between particles (molecules) to statistical distributions of relative particle positions[8]. In our statistical–mechanical analysis we have used the pair distribution function, $g(r)$, which is a measure of the frequency of finding a second particle at a point a distance r away from a given first one. Previous studies of electron micrographs to determine interactions between membrane proteins have been limited to analyses of $g(r)$[9–11]. As $g(r)$ does not in practice uniquely determine the pair force, these studies have necessarily been qualitative and indirect.

To overcome this difficulty, we have in addition used a triplet distribution function, $\rho(s, \theta; r)$, which measures the frequency of encountering a particle at polar coordinates (s, θ) with respect to a given pair of particles separated by r. (See the insert in Fig. 1 for the coordinate system.)

The relation between the pair and triplet functions and the effective force between pairs of particles, $f(r)$, is given by the Born–Green–Yvon (BGY) equation[8]:

$$kT\frac{\mathrm{d}[\ln(g(r))]}{\mathrm{d}r} = f(r) + \int_0^\infty \int_0^{2\pi} f(s)\cos(\theta)\rho(s, \theta; r)s\,\mathrm{d}\theta\,\mathrm{d}s \quad (1)$$

The left-hand side of the BGY equation may be seen to represent the statistical mean force, $F(r)$, acting on a particle when there is a second particle a distance r away by relating $g(r)$ to a potential, $W(r)$, according to the Boltzmann distribution, $g(r) \equiv \exp(-W(r)/kT)$; then

$$F(r) \equiv -\frac{\mathrm{d}(W(r))}{\mathrm{d}r} = kT\frac{\mathrm{d}[\ln(g(r))]}{\mathrm{d}r} \quad (2)$$

The BGY equation states that this total force arises from two sources: the direct force between the two particles, $f(r)$, and the forces from all other particles (the integral). The integrand weights the component along r of the force exerted on the first particle from these other particles, $f(s)\cos(\theta)$, by their average number at (s, θ), $\rho(s, \theta; r)$. The integral extends over the whole membrane, but contributions to it are small for s larger than a few molecular diameters.

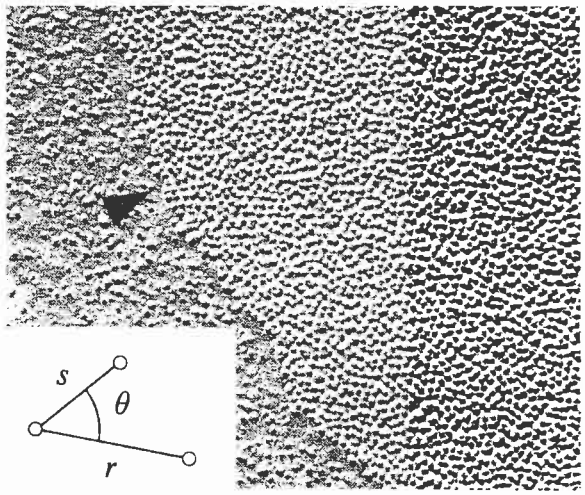

Fig. 1 Freeze-fracture electron micrograph of part of a gap junction from mouse liver, in the open conducting state. This micrograph was made as part of a study by Raviola *et al.*[4]. The gap-junction proteins are seen to be aggregated into a plaque (arrow), at a density of 9,330 particles per μm^2 and an average separation of ~10 nm. Particles of similar size in the neighbouring membrane are much more disperse. The inset shows the polar coordinate system used in the analysis of triplet molecular distributions.

The integral over θ can be performed as part of the data acquisition; this reduces the term to a function of r and s that is then tabulated over bins of non-zero width (the integral over s is then approximated as a Riemann sum). The BGY equation reduces to a system of linear equations with the tabulated force as its unique solution. Tabulating the many triplet configurations is a formidable computational task, but it can be made manageable by using suitable algorithms (J.B., J.R.A. and J.C.O., in preparation). To test our method, we performed a Monte Carlo simulation of a simple two-dimensional fluid and recovered the correct forces (attractions as well as repulsions) from samples of the molecular positions (J.B., J.R.A. and J.C.O., in preparation). For the gap junction, the calculated force contains the influences of unobserved degrees of freedom (for example, lipid positions and dyad orientations) and multi-body interactions among dyads in an averaged manner. To reflect this fact, we refer to it as an effective pair force.

Figure 2 shows $g(r)$ calculated for the dyads in the plaque in Fig. 1. Its functional shape is typical of simple fluids. The calculated force between dyads, given in Fig. 3, is entirely repulsive (that is, positive); its range is ~12 nm, well beyond the distance at which dyads are in direct contact, which we estimate at no more than 7 nm, based on electron microscopy[12]. Several contributions to this force are conceivable, including the effects of intervening lipids. However, volume exclusion at 5–6 nm, together with electrostatic repulsion due to the order of 10 elementary charges per dyad, provides the simplest and best quantified accounting of the observed force; it is also consistent with the suggestion[7] that the tighter aggregation and crystallization observed when the dyads bind cations and close their pores is due to a reduction of electrostatic repulsion.

The fact that our analysis leads to a simple, physically interpretable force is in itself significant. If the distribution of dyad positions were the result of cytoskeletal anchoring, the calculated force would probably be highly unphysical. Our results thus provide additional evidence that gap junctions represent the equilibrium state of dyads and reflect the forces that act between them. At the same time, our result rules out effective attractions between individual dyads (such as the proposed

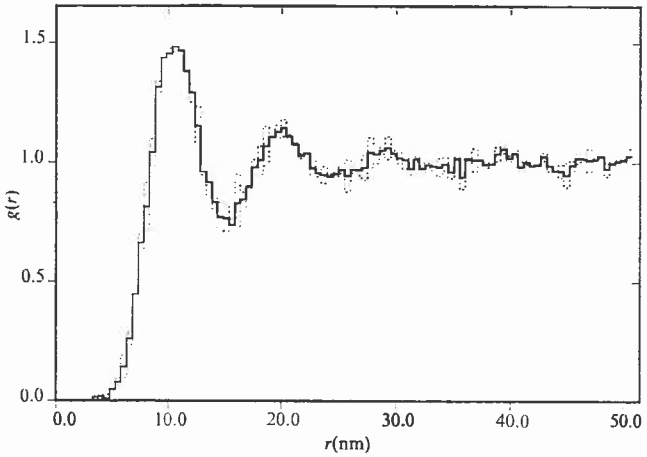

Fig. 2 Pair distribution function, $g(r)$, for dyads inside the plaque in Fig. 1. The uncertainties in digitizing the positions of the centres of the dyads lie in the range 0.5–1.0 nm. The error envelope (dotted line) represents the standard deviations obtained by performing the analysis separately on two parts of the plaque, containing a total of 4,319 dyads. Information contained in $g(r)$ includes the effective diameter of the dyads (the range where $g(r)$ is close to 0), the predominant first neighbour separation (the position of the first peak), and the radial decay of order in successive shells of neighbours about each dyad (the damped oscillatory behaviour of $g(r)$).

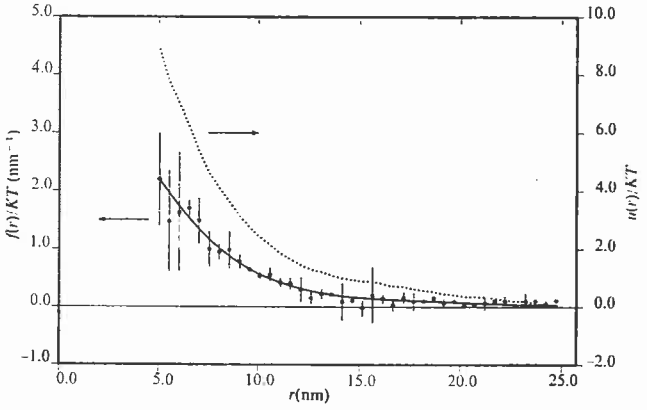

Fig. 3 Effective pair force, $f(r)$ (●), between dyads in the plaque in Fig. 1, computed using the BGY equation. The force was divided by the thermal Boltzmann energy, kT, where $T \sim 310$ K. The error bars for the force were obtained as in Fig. 2. In the range 25–50 nm (not shown) the force is small; the extremes are -0.21 and $+0.17$ nm^{-1}, with error bars ~ 0.1 nm^{-1}. Considering the statistical fluctuations in the data and the accuracy of the numerical methods, there is little evidence that the true force differs significantly from zero in the extended range. The dotted line shows the effective pair potential, $u(r)$, obtained by integrating the force over r; this is the pair energy required to compress two dyads from a reference separation of 25 nm in the plaque.

specific binding between gap-junction proteins)[2] that could have explained why dyads are aggregated in plaques. One can, however, imagine several ways in which dyads could aggregate without pair attractions acting inside the plaque. Such mechanisms might arise from the bending elasticity of membranes[1] or from attractions between proteins due to perturbations of nearby lipids[13–15].

The mechanism that we find most satisfactory is illustrated schematically in Fig. 4: when a dyad is formed by linking gap-junction proteins in two apposed membranes, surrounding areas of membrane are drawn to within 2 nm of each other[16]. In the process, the mutual repulsion of the membranes, partly

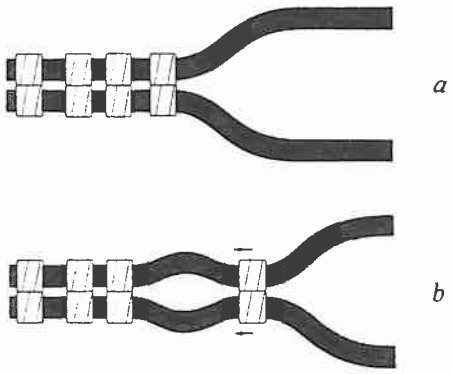

Fig. 4 Hypothetical mechanism of dyad cohesion (schematic). The escape of a dyad from an aggregate ($a \rightarrow b$) increases the area of energetically unfavourable close apposition of the membranes. This provides the driving force for the cohesion. For dyads within the aggregate, however, the force largely vanishes.

electrostatic in nature, must be overcome[17]. The total energy expended in overcoming this repulsion is minimized when the area of close apposition is minimized—that is, when the dyads aggregate. We estimate that the electrostatic repulsions alone are sufficiently strong to maintain the observed density of dyads (J.B., J.R.A. and J.C.O., in preparation).

The total area of closely apposed membrane would, however, be largely independent of the positions of the individual dyads in the junction. Accordingly, dyads in the bulk of the junction would not experience this attraction. Isolated pairs of dyads would experience it, as would dyads crossing the boundary of the junction.

This mechanism requires that the two halves of a dyad be bonded quite strongly. The apposed halves of gap junctions are, in fact, difficult to separate[18].

Our model can also explain certain aspects of the formation and disassembly of gap junctions: the formation of conducting dyads precedes the appearance of aggregates of intramembrane particles in Novikoff hepatoma cells that have been dispersed and then allowed to reaggregate[19]. In the same system, disperse assemblies of intramembrane particles appear to develop into aggregated ones[18]. After dissociation of the cells, gap junctions in which the second membrane is still present (albeit torn loose from its cell) remain intact for some time, whereas intramembrane particle assemblies apparently disperse where dyads have been split[18].

Based on our knowledge of the effective force with which dyads interact, we have outlined how gap junctions may maintain their structure: dyads that repel each other remain aggregated because of a requirement to minimize the area where membranes approach each other closely. Finally, we note that gap junctions vary considerably among tissues and species[1,2]. It remains to be seen to what extent the forces that we have observed in a mouse liver gap junction operate elsewhere.

We acknowledge the generous gift of micrographs by E. Raviola, as well as computer access by D. Glaser and R. Henry. This work was supported by grants from the NIH (B.R.S.G. 2-S07-RR07006) and the American Chemical Society/Petroleum Research Fund (12378-G6). J.B. is a fellow of the German National Fellowship Foundation, and J.R.A. is a NIH predoctoral trainee.

Received 30 December 1983; accepted 3 May 1984.

1. Loewenstein, W. R. *Physiol. Rev.* **61**, 829–913 (1981).
2. Bennett, M. V. L. & Goodenough, D. A. *Neurosci. Res. Prog. Bull.* **16**, 415 (1978).
3. Heuser, J. E. & Reese, T. S. in *The Neurosciences Fourth Study Program* (eds Schmitt, F. O. & Worden, F. G.) (MIT Press, Cambridge, Massachusetts, in the press).
4. Raviola, E., Goodenough, D. A. & Raviola, G. *J. Cell Biol.* **87**, 273–279 (1980).
5. Meller, K. *Anat. Embryol.* **163**, 321–330 (1981).
6. Tadvalkar, G. & Pinto da Silva, P. *J. Cell Biol.* **96**, 1279–1287 (1983).
7. Peracchia, C. & Peracchia, L. L. *J. Cell Biol.* **87**, 719–727 (1980).
8. Hill, T. L. *Statistical Mechanics* Ch. 6 (McGraw-Hill, New York, 1956).
9. Markovics, J., Glass, L. & Maul, G. G. *Expl Cell Res.* **85**, 443–451 (1974).
10. Perelson, A. S. *Expl Cell Res.* **112**, 309–321 (1978).

11. Pearson, T. L., Chan, S. I., Lewis, B. & Engelman, D. M. *Biophys. J.* **43**, 167–174 (1983).
12. Unwin, P. N. T. & Zampighi, G. *Nature* **283**, 545–549 (1980).
13. Marcelja, S. *Biochim. biophys. Acta* **455**, 1–7 (1976).
14. Owicki, J. C. & McConnell, H. M. *Proc. natn. Acad. Sci. U.S.A.* **76**, 4750–4754 (1979).
15. Edelman, J. B. thesis, California Inst. Technol., Pasadena (1978).
16. Goodenough, D. A. *Cold Spring Harb. Symp. quant. Biol.* **40**, 37–43 (1976).
17. Rand, R. P. *A. Rev. Biophys. Bioengng* **10**, 277–314 (1981).
18. Preus, D., Johnson, R. & Sheridan, J. *J. ultrastruct. Res.* **77**, 248–262 (1981).
19. Johnson, R., Hammer, M., Sheridan, J. & Revel, J. P. *Proc. natn. Acad. Sci. U.S.A.* **71**, 4536–4540 (1974).